Electronic Supplementary Material (ESI) for Nanoscale Advances.
This journal is © The Royal Society of Chemistry 2021

Supplementary Information: The interaction of size-selected Ru_3 clusters with RF-deposited TiO_2: probing Ru-CO binding sites with CO-TPD

Liam Howard-Fabretto[1,2], Timothy J. Gorey[3], Guangjing Li[3], Siriluck Tesana[4], Gregory F. Metha[5], Scott L. Anderson[3], and Gunther G. Andersson[1,2]*

1 Flinders Institute for Nanoscale Science and Technology, Flinders University, Adelaide, South Australia 5042, Australia

2 Flinders Microscopy and Microanalysis, College of Science and Engineering, Flinders University, Adelaide, South Australia 5042, Australia

3 Chemistry Department, University of Utah, 315 S. 1400 E., Salt Lake City, UT 84112, United States

4 The MacDiarmid Institute for Advanced Materials and Nanotechnology, School of Physical and Chemical Sciences, University of Canterbury, Christchurch 8141, New Zealand

5 Department of Chemistry, University of Adelaide, Adelaide, South Australia 5005, Australia

*Corresponding author: Gunther G. Andersson

Email: gunther.andersson@flinders.edu.au.

Address: Physical Sciences Building (2111) GPO Box 2100, Adelaide 5001, South Australia

Cluster Depositions

Cluster Source Depositions (Utah)

Ru_3 clusters were produced under UHV using a cluster source (CS) by pulsed laser vaporisation of a 99.9% pure Ru target. Vaporised target atoms were pulsed into a helium gas flow, followed shortly by supersonic expansion of the Ru into the vacuum. A radio frequency (RF) quadrupole ion guide was set to collect only positively charged clusters, and the cluster beam was angled by 20° to remove neutral clusters which cannot be electrostatically size-selected. The beam passed through several differential pumping stages, before reaching a quadrupole mass filter which can select for a specific mass/charge ratio. Because most clusters are singly changed [1, 2] this can be treated as cluster mass selection where only a single size of cluster is selected for passing through the quadrupole. A 2 mm diameter aperture positioned 1 mm from the surface ensured the cluster spot was approximately 2 mm in diameter. A retarding potential was used to ensure a deposition energy of ~1 eV/atom, to prevent fragmentation upon cluster impact [3].

For each cluster source deposition, the substrates were liquid N_2 cooled to 180 K, followed by a quick temperature flash to 700 K to remove any adventitious hydrocarbons which may have adsorbed from the vacuum chamber while the sample was cooling. After flash heating the samples were left to cool, and the cluster depositions were initiated at 300 K, and continued as the sample cooled to 180 K. For each cluster source deposition 1.5 x 10^{14} Ru atoms/cm^2 were deposited. Clusters were neutralised when deposited due to the conductivity of both the RF-TiO_2 and the SiO_2 substrates. The neutralisation current was measured and summed during deposition to keep the amount of deposited cluster material consistent.

Each CS deposition in this study followed the same procedure, except for the pre-deposition treatment process. RF-TiO_2 samples were heated under UHV to 723 K for 10 minutes to remove surface hydrocarbons. The surface was then Ar^+ sputtered to the required dosage (except for NS-RF-TiO_2 which was not sputtered), and clusters were deposited with the cluster source. For the deposition onto SiO_2 the initial heating step was different; SiO_2 was heated to 700 K for 20 minutes under an atmosphere of 7 x 10^{-6} mbar O_2 to preserve the surface oxide layer, followed by a further 2 minutes of heating under UHV.

Chemical Vapor Deposition (Adelaide)

For chemical vapor deposition (CVD), a sample vial with 2.13 mg ± 0.05 mg of $Ru_3(CO)_{12}$ was loaded into the vacuum chamber on a manipulator arm which could be extended such that the vial directly faced the substrate at a distance of <1 cm. $Ru_3(CO)_{12}$ depositions were performed with the clusters and substrate at room temperature, where the starting pressure was <7 x 10-

[7] mbar.

A full CVD sample preparation procedure was performed as follows: RF-TiO_2 was heated under UHV to 723 K for 10 minutes then sputtered with Ar^+ at 6 x 10^{14} doses/cm^2. $Ru_3(CO)_{12}$ was deposited by CVD in the loading chamber for 120 minutes, and the cluster-deposited sample was then removed from the vacuum for transferring to the main UHV apparatus.

List of Samples

A list of all cluster samples analysed in the study is given below in Table S1. All samples were prepared in Utah, except for CVD-deposited $Ru_3(CO)_{12}$/HDS-RF-TiO_2, which was prepared *ex situ* in Adelaide. All CO-TPD and XPS were performed in Utah. Some samples were analysed with both CO-TPD and XPS, while some were analysed by one technique only. Multiples of the same sample were prepared in some cases to allow for further XPS testing. For CO-TPD, blank measurements were performed on each substrate prior to cluster depositions, except for $Ru_3(CO)_{12}$/HDS-RF-TiO_2. The treatment of the samples for the XPS measurements are shown in the table. The blank XPS measurements in the main text were performed on same cluster samples, prior to cluster depositions.

Table S1: List of samples analysed with CO-TPD and XPS.

Deposition	Substrate	Analysis Techniques	XPS Measurements Performed
CS Ru_3	SiO_2	CO-TPD	N/A
CS Ru_3	SiO_2	XPS	No treatment, and 800 K
CS Ru_3	NS-RF-TiO_2	CO-TPD and XPS	No treatment, and 800 K
CS Ru_3	NS-RF- TiO_2	XPS	No treatment, and after CO dose
CS Ru_3	LDS-RF-TiO_2	CO-TPD	N/A
CS Ru_3	HDS-RF- TiO_2	CO-TPD and XPS	800 K, and after CO dose.
CVD $Ru_3(CO)_{12}$	HDS-RF- TiO_2	CO-TPD and XPS	No treatment, 800 K heating, and after CO dose.

Data Analysis

CO-TPD

The CO-TPD calibration used the QMS counts resulting from a known flux of CO added to the

chamber at the end of each experiment. It was performed according to the procedure reported by Li *et al.* [4], using the same instrument. The real measurement time (duty factor) for each mass monitored during the QMS cycles was corrected for. The fact that the skimmer cone was 2.5 mm in diameter and the cluster spot was 2 mm in diameter contributes an uncertainty to this calculation; angular distribution effects may affect the efficiency of detection depending on the distance of the sample to the aperture. Due to this it was estimated that the accuracy of the absolute TPD intensity calibration was ~50%, while the relative uncertainty between samples was ~15%.

A procedure was used to integrate the CO-TPD desorption spectra over time, to determine the total number of CO molecules desorbed. The integration was estimated by dividing the desorption spectrum into many thin, right angle trapezoids and calculating the total area. For CS depositions a known number of cluster atoms were deposited, and the total CO desorbing per cluster atom was determined. However, for CO-TPD spectra of Ru clusters on RF-TiO_2 substrates the largest Ru-CO desorption feature overlapped with a background signal due to the sample holder degassing at ~750 K. Thus, these spectra could not be integrated without assuming their shape beyond 750 K. The only CO-TPD measurement for which the integration was performed was for Ru_3/SiO_2. The absolute error in the reported CO desorbing per Ru atom was assumed to be the same as the CO desorption rate; ~50% absolute error and ~15% relative error when comparing between measurements.

XPS

CasaXPS was used to model XPS spectra. Peaks were typically fitted using the symmetrical GL(30) line shape, which is a convolution of Gaussian and Lorentzian line shapes. Shirley backgrounds were subtracted from each raw spectrum when integrating the fitted peaks [5]. Binding energies were calibrated to C 1s = 285.0 eV. The binding energy accuracy of the XPS instrument for peak locations is ± 0.2 eV when comparing different samples, and ± 0.1 eV when comparing the same sample after surface treatment. Every XPS spectrum featured C 1s peaks related to contamination to some extent. Two peaks were always present, due to C-C or C-H bonding at 285.0 eV, and C=O or C-O-C bonding at 287.0 eV. A third carbon peak at 289.4 eV, likely due to O=C-O bonding was sometimes present but was most often removed by UHV heat treatment and/or sputtering. These compare to previously reported assignments for carbon contamination on SiO_2 substrates [6].

Care was paid when fitting the Ru 3d doublet for clusters. This was because the 285.0 eV adventitious C 1s peak overlapped with the Ru 3d doublet. There was often partial overlap with the Ru $3d_{5/2}$ peak, and the Ru $3d_{3/2}$ was typically completely covered due to the low Ru surface coverages. To aid with fitting the covered Ru $3d_{3/2}$ peak, an Ru reference metal was

fitted and used to determine constraints. When comparing the $3d_{5/2}$ to $3d_{3/2}$ peaks, the peak separation was 4.17 eV, peak area ratio was 3:2, and FWHM ratio was 1:1.15. For Ru cluster XPS peak fitting, these values were used to lock the size and shape of the $3d_{3/2}$ peak to the $3d_{5/2}$ peak which as be more easily fitted. The reason the FWHM of the Ru $3d_{3/2}$ peak was larger than the $3d_{5/2}$ was due to a Coster-Kronig broadening effect for the $3d_{3/2}$ peak [7, 8].

Ru peaks were fitted with asymmetrical line shapes; it is typical for transition metals such as Ru to feature asymmetrical line shapes for the 3d core electrons, and work has been done by Morgan [8] investigating the best way to fit this asymmetry for Ru in different chemical environments. The extent of the peak asymmetry is dependent on the chemical nature of the Ru, and the measured asymmetry may also be effected by the resolution of the XPS instrumentation [7-9]. A modified version of the line shape used by Morgan for metallic Ru was used to fit the previously mentioned Ru reference sample XPS data, where Ru $3d_{5/2}$ used LF(0.8,1.3,500,180) and Ru $3d_{3/2}$ used LF(1.15,1.5,500,50). The LF line shape corresponds to a "Lorentzian asymmetric line shape with tail damping" in CasaXPS. To the best of our knowledge, there are no published asymmetry results for Ru in cluster form, and thus the line shapes published by Morgan were used as a starting point and were altered to best fit the line shape seen for the Ru clusters. These line shape parameters are shown in Table S2 below. A special case was for as-deposited, $Ru_3(CO)_{12}$ clusters; these were fitted with symmetrical GL(30) line shapes.

Table S2: Line shapes used for fitting Ru 3d peaks from XPS in different scenarios. LF means Lorentzian asymmetric line shapes with tail damping, while GL means a convolution of Gaussian and Lorentzian line shapes.

Measurement	**Ru $3d_{5/2}$ line shape**	**Ru $3d_{3/2}$ line shape**
Metallic Ru reference sample	LF(0.8,1.3,500,180)	LF(1.15,1.5,500,50)
Ru clusters	LF(0.7,1.8,25,280)	LF(0.7,1.8,25,280)
As-deposited, Ligated Ru clusters	GL(30)	GL(30)

Atomic concentrations in percentage (At%) were determined using XPS by fitting all peaks, integrating the peaks to determine their area, and then calibrating the areas by dividing them by the XPS sensitivity factors found in the Handbook of X-ray Photoelectron Spectroscopy [10]. Ratios of individual elements to the total peak area were multiplied by 100% to determine At%. Due to the information depth of XPS, the At% represents an average of the atomic

concentration over the top several layers of the sample, with the average being weighted towards upper layers for which there are a higher probability of photoelectrons reaching the detector. The relative resolution for At% varied depending on the size of the peaks, and whether they overlapped with other peaks. Due to this, the relative fitting uncertainty in At% for each peak of interest was estimated by determining the largest range of peak areas which resulted in what was considered to be a reasonable fitting of the measured spectra. The relative uncertainty for Ru At% of deposited cluster peaks was ~4%. For substrate materials, the relative At% uncertainty for Ti^{4+} 2p, O 1s, and Si 2p in SiO_2 and RF-TiO_2 substrates were each ~1%. The defects in RF-TiO_2 substrates are present as Ti^{3+}, and these each have a relative uncertainty of ~24%; this is greater than Ti^{4+} 2p because they are on a shoulder of the larger Ti^{4+} peak. The fitting procedure was kept consistent for all Ti 2p spectra to minimise the relative error, and as such it was estimated that the relative uncertainty in the Ti^{3+} At% when comparing between the samples was lower at ~15%. For Ti^{3}/Ti^{Total} ratios, the ~15% Ti^{3+} 2p fitting uncertainty was taken to be the dominant uncertainty.

The surface coverage of cluster material was estimated for each cluster deposition where XPS was performed. The surface coverages are presented in units of % ML, which is the percentage relative to an entire monolayer of coverage. This estimation was done using a calculation procedure similar to that used by Eschen *et al.* [11], except for a difference that Eschen *et al.* used multiple XPS detection angles. This calculation solved for the surface concentration required to achieve the measured XPS At% for Ru. The clusters were assumed to be present in only a single monolayer on the surface with negligible stacking of atoms and no mixing of cluster and substrate layers. The Ru-Ru bulk interatomic distance of 0.265 nm [12] was used as an estimate of the layer thickness for deposited Ru. The contribution of individual atoms to the XPS spectra will be reduced as the depth of the atom into the surface increases, and this was factored into the calculation using the in elastic mean free path (IMFP) of electrons in TiO_2. An IMFP of 1.8 nm was used based on a study which calculated the IMFP of electrons in thermally grown TiO_2 based on experimental measurements at an excitation energy of 1250 eV [13]. The IMFP changes with excitation wavelength as well as substrate material, however for consistency was kept at 1.8 nm for all calculations including those based on measurements using an SiO_2 substrate.

A range of factors contribute to the uncertainty in surface coverage estimations. These include errors in the calculated XPS At% for the clusters, differences between atomic sensitivity factors in our detector setup and in the XPS handbook [10], and any inaccuracy in the IMFP of electrons in the substrate. Inaccuracies in the IMFP could be based on structural differences between the RF-TiO_2 used this study and the reference study for IMFP, differences between

the IMFP between RF-TiO_2 and SiO_2, and differences in the exact excitation wavelength used. Based mainly on the uncertainty of the IMFP, the absolute error in surface coverage estimates was assumed to be ~100%. However, the relative error comparing between samples only comes from the cluster At% fitting uncertainty and was ~4%. While the ~100% error can be considered high, for relative comparisons between samples the results were deemed reliable. Additionally, the surface coverage estimation was intended to give the scale for the surface coverage of clusters used in the experiments, rather than determining the exact coverage.

Results

Metallic Ru Reference Sample

Figure S1 shows the XPS spectrum for the Ru 3d region of a Ru reference sample, which was fitted with one asymmetrical Ru doublet. The Ru $3d_{5/2}$ peak is located at 279.7 eV ± 0.2 eV and the doublet peak separation is 4.17 eV. This is comparable to the Ru $3d_{5/2}$ BE reported by Morgan [8] for metallic Ru at 279.75 eV.

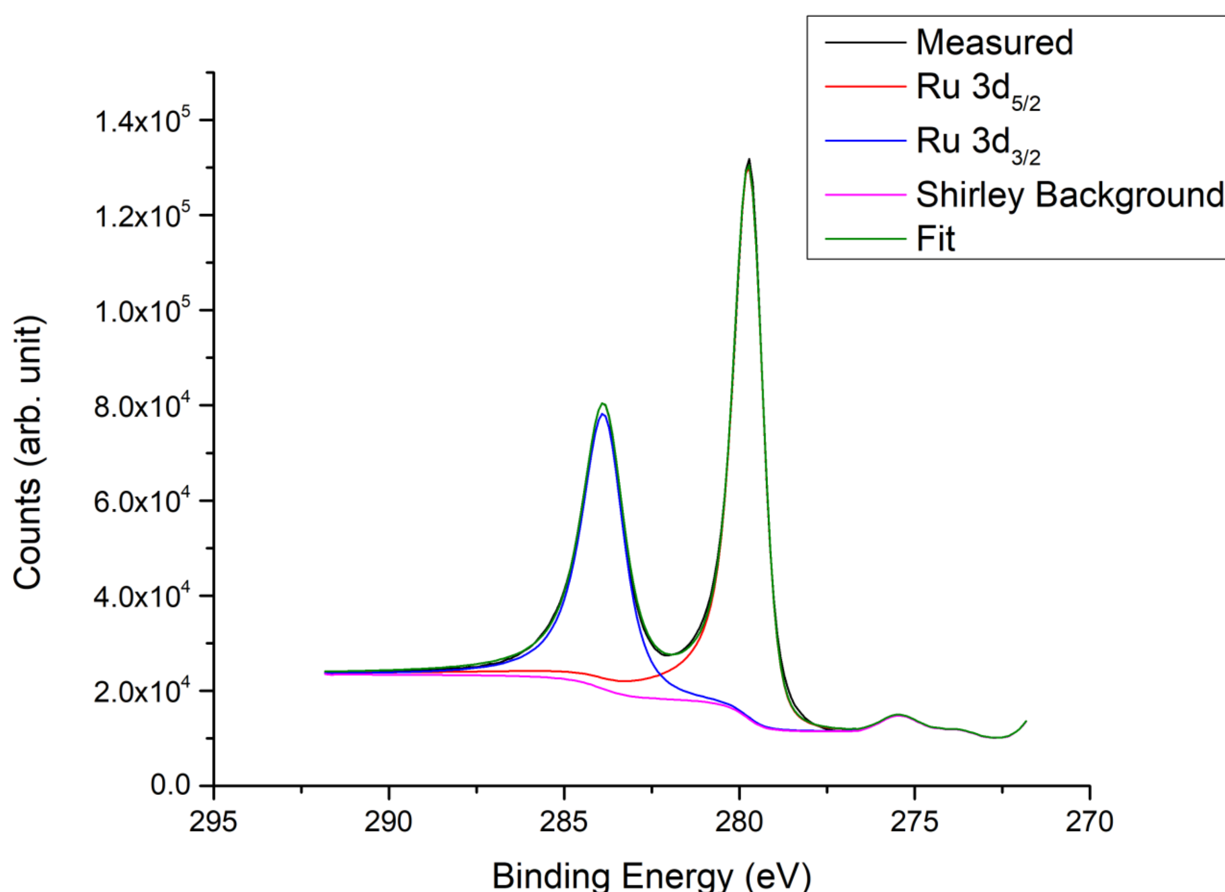

Figure S1: XPS results for Ru metallic reference sample - Ru 3d region peak fitting. Measurement was after heating the sample to 1073 K and sputtering for 1 hour to remove hydrocarbon contamination and surface Ru oxides.

Ti 2p Region – Surface Defects

Less than 5% Ti^{3+}/Ti^{Total} is considered as negligible surface defects. The ~15% uncertainty in the Ti^{3+}/Ti^{Total} ratio was estimated due to fitting the Ti^{3+} peak on the shoulder of the larger Ti^{4+} peak, in addition to the changing background signal in the Ti 2p region.

Ti^{3+}/Ti^{Total} ratios are given in Table 3 of the main text. The Ti^{3+}/Ti^{Total} ratio is 6% ± 15% for blank NS-RF-TiO_2 after heating to 800 K. This shows that defects were present to some extent on non-sputtered TiO_2. The level of defects in the blank NS-RF-TiO_2 at 800 K was greater than when bare Ru_3 was deposited on the same type of substrate; this can be attributed to the clusters preferentially binding to the Ti^{3+} defect sites on the surface [47, 48], which decreases the amount of Ti^{3+}. There is no significant change in the Ti^{3+}/Ti^{Total} ratio for Ru_3/NS-RF-TiO_2 upon heating to 800 K. The Ti^{3+}/Ti^{Total} ratio of Ru_3/HDS-RF-TiO_2 at 800 K was 11% ± 15%, greater than that of all other samples. The greater number of defects was expected due to the pre-deposition Ar^+ sputtering process. For $Ru_3(CO)_{12}$/HDS-RF-TiO_2, the Ti^{3+}/Ti^{Total} ratio was only 4% ± 15% after heating to 800 K; this was lower than expected for bare Ru_3 on the same type of substrate. This was likely due to a combination of the ~3 times greater surface coverage of $Ru_3(CO)_{12}$ passivating the Ti^{3+}, in addition to some defect passivation from atmospheric exposure which could not be reversed by heating to 800 K.

CO/Ru Ratio for $Ru_3(CO)_{12}$/HDS-TiO_2 Sample

The CO/Ru ratio for the as-deposited $Ru_3(CO)_{12}$/HDS-TiO_2 sample was estimated using the XPS At% data for Ru 3d and CO 1s peaks, shown in Table S3. The results in are from an *in situ* XPS measurement of the sample performed at Flinders University. Note that this sample was also used for CO-TPD and XPS in the main text (e.g. the results in Figure 2). The At% for CO 1s present on the sample before the CVD deposition (but after heating and sputtering the substate) was subtracted from the CO 1s At% after the deposition, to take into account any adventitious CO contamination present on the substrate. The ratio between the CO 1s At% and the Ru 3d At% was determined to be ~1.3. Based on this, the approximate formula of the clusters (as-deposited) for the $Ru_3(CO)_{12}$/HDS-TiO_2 sample is $Ru_3(CO)_4$. However, the atomic ratio should be taken as an estimation because it may be affected by signal due to any adventitious carbon added during the CVD deposition process.

Table S3: XPS data for the $Ru_3(CO)_{12}$/HDS-TiO_2 sample. The At% of CO 1s and Ru 3d are presented to determine the CO/Ru ratio. CO 1s results are given before and after the deposition, and the difference was calculated.

Sample	CO 1s At% - before CVD (%)	CO 1s At% - after CVD (%)	CO 1s At% - difference (%)	Ru 3d At% - after CVD (%)	CO/Ru ratio
$Ru_3(CO)_{12}$/HDS-TiO_2	0.3	2.5	2.2	1.8	1.3

References

[1] H. Haberland, Mall, M., Moseler, M., Qiang, Y., Reiners, T., and Thurner, Y., Filling of micron-sized contact holes with copper by energetic cluster impact, J. Vac. Sci. Technol. A 12 (1994) 2925-2930.
[2] H. Haberland, Karrais, M., Mall, M., and Thurner, Y., Thin films from energetic cluster impact: A feasibility study, J. Vac. Sci. Technol. A 10 (1992) 3266-3271.
[3] V.N. Popok, I. Barke, E.E.B. Campbell, K.-H. Meiwes-Broer, Cluster–surface interaction: From soft landing to implantation, Surf. Sci. Rep. 66 (2011) 347-377.
[4] G. Li, B. Zandkarimi, A.C. Cass, T.J. Gorey, B.J. Allen, A.N. Alexandrova, S.L. Anderson, Sn-modification of Pt7/alumina model catalysts: Suppression of carbon deposition and enhanced thermal stability, J. Chem. Phys. 152 (2020) 024702.
[5] J. Castle, A. Salvi, Chemical state information from the near-peak region of the X-ray photoelectron background, J. Electron. Spectrosc. Relat. Phenom. 114 (2001) 1103-1113.
[6] E.L. Strein, D. Allred, Eliminating carbon contamination on oxidized Si surfaces using a VUV excimer lamp, Thin Solid Films 517 (2008) 1011-1015.
[7] Y.J. Kim, Y. Gao, S.A. Chambers, Core-level X-ray photoelectron spectra and X-ray photoelectron diffraction of RuO2 (110) grown by molecular beam epitaxy on TiO2 (110), Appl. Surf. Sci. 120 (1997) 250-260.
[8] D.J. Morgan, Resolving ruthenium: XPS studies of common ruthenium materials, Surf. Interface Anal. 47 (2015) 1072-1079.
[9] J. Riga, C. Tenret-Noel, J.-J. Pireaux, R. Caudano, J. Verbist, Y. Gobillon, Electronic structure of rutile oxides TiO2, RuO2 and IrO2 studied by X-ray photoelectron spectroscopy, Phys. Scr. 16 (1977) 351.
[10] J. Chastain, Handbook of X-ray photoelectron spectroscopy, Perkin-Elmer Corporation, Minnesota, USA, 1992, pp. 221.
[11] F. Eschen, M. Heyerhoff, H. Morgner, J. Vogt, The concentration-depth profile at the surface of a solution of tetrabutylammonium iodide in formamide, based on angle-resolved photoelectron spectroscopy, J. Phys. Condens. Matter 7 (1995) 1961.
[12] L. Sutton, Tables of interatomic distances and configuration in molecules and ions, Chemical Society1965.
[13] G. Fuentes, E. Elizalde, F. Yubero, J. Sanz, Electron inelastic mean free path for Ti, TiC, TiN and TiO2 as determined by quantitative reflection electron energy-loss spectroscopy, Surf. Interface Anal. 33 (2002) 230-237.